University of
Strathclyde
Glasgow

Strathprints Institutional Repository

PERFORMANCE LIMITATIONS OF SUBBAND ADAPTIVE FILTERS

S. Weiß, R.W. Stewart

Signal Processing Division, Dept. of EEE
University of Strathclyde
Glasgow G1 1XW, Scotland
{weiss,bob}@spd.eee.strath.ac.uk

A. Stenger, R. Rabenstein

Lehrstuhl für Nachrichtentechnik
Universität Erlangen-Nürnberg
Erlangen, Germany
{stenger,rabe}@nt.e-technik.uni-erlangen.de

ABSTRACT

In this paper, we evaluate the performance limitations of subband adaptive filters in terms of achievable final error terms. The limiting factors are the aliasing level in the subbands, which poses a distortion and thus presents a lower bound for the minimum mean squared error in each subband, and the distortion function of the overall filter bank, which in a system identification setup restricts the accuracy of the equivalent fullband model. Using a generalized DFT modulated filter bank for the subband decomposition, both errors can be stated in terms of the underlying prototype filter. If a source model for coloured input signals is available, it is also possible to calculate the power spectral densities in both subbands and reconstructed fullband. The predicted limits of error quantities compare favourably with simulations presented.

1 INTRODUCTION

Adaptive filtering in subbands is widely used for problems where an adaptive system is required to identify very long impulse responses, since it enables to process in decimated subbands with decreased complexity [4, 2], which is e.g. exploited in acoustic echo cancella-
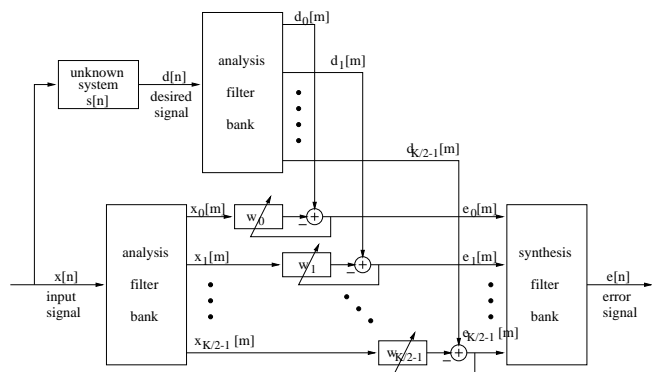

Fig. 1: Subband adaptive filter structure in a system identification setup.

tion. Performance characteristics of subband adaptive

filters (SAF) as shown in Fig. 1 due to the subband splitting have mainly been addressed in terms of convergence speed. Investigations into the achievable final convergence errors are mainly made in terms of truncation errors and non-causality [4, 9], while there are little hints for the influence of distortions introduced by the filter banks [5, 8].

In the following, we discuss convergence error limits of subband adaptive filtering in dependency on a generalized DFT (GDFT) modulated filter bank used for subband decomposition, which will be briefly reviewed in Sec. 2. In Sec. 3, we then introduce a method to obtain the power spectral density (PSD) of the aliasing terms, which sets the lower limit for the adaptation error. This limit can be approximated by a stopband attenuation measure of the prototype filter. A second part then discusses the error inherent in the fullband model of the adapted subband filters. Simulations supporting our results are presented in Sec. 4.

2 GDFT MODULATED FILTER BANKS

2.1 Modulation

A general structure of a K band filter bank with decimation by a factor $N \leq K$ is shown in Fig. 2. The analysis filters $h_k[n]$ are derived from a real valued lowpass prototype FIR filter $p[n]$ of length L_p by a generalized discrete Fourier transform (GDFT),

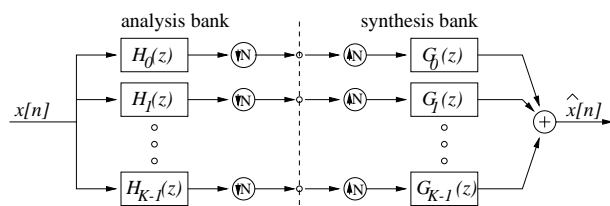$$ h_k[n] = e^{j \frac{2\pi}{K}(k+k_0)(n+n_0)} \cdot p[n], \qquad k, n \in \mathbb{N}. \qquad (1) $$

Fig. 2: Analysis and synthesis branch of a K-channel filter bank with subbands decimated by N.
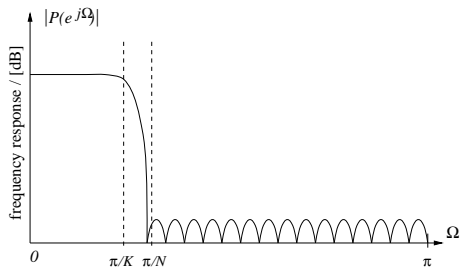
Fig. 3: Required frequency response of the real valued prototype filter $p[n]$ for a K channel oversampled GDFT filter bank with decimation by N.

The term generalized DFT [1] stems from offsets k_0 and n_0 introduced into the frequency and time indices. With $k_0 = 1/2$, it is sufficient for real valued input $x[n]$ to process the first $K/2$ subbands covering the frequency interval $[0; \pi]$, while the remaining subbands are redundant. Together with conditions on $p[n]$, the time offset n_0 can be set appropriately to ensure useful properties such as linear phase. The synthesis filters $g_k[n]$ can be obtained by time reversal and complex conjugation of the analysis filters, i.e. $g_k[n] = \tilde{h}_k[n] = h_k^*[L_p - n + 1]$. The modulation approach allows for both low memory consumption for storing filter coefficients and an efficient polyphase implementation [7].

2.2 Prototype Design

Through the above modulation, the filter bank design reduces to an appropriate choice of the prototype filter, which has to fulfill two criteria. Firstly, the filters' attenuation in the stopband ranging from $[\pi/N; \pi]$, as indicated in Fig. 3, has to be sufficiently large. Every frequency of the input signal in the interval $[\pi/N; \pi]$ will be aliased into the baseband after filtering and decimation, and cause a distortion of the subband signal.

A second constraint on the design is the perfect reconstruction condition. If stopband attenuation of the prototype filter is high enough to sufficiently suppress aliasing, this condition reduces to the consideration of inaccuracies in power complementarity [6]:

$$\sum_{k=0}^{K-1} |H_k(e^{j\Omega})|^2 \overset{!}{=} 1. \qquad (2)$$

A prototype filter approximating these constraints can be constructed by an iterative least-squares method [7].

3 PERFORMANCE LIMITATIONS

In this section, we derive limitations in adaptation assuming that the only disturbance originates from the filter banks employed for the subband decomposition. First, we look at the achievable error PSD and the mean squared error (MSE) term, $\mathcal{E}\{e^2[n]\}$, which is important to minimize in e.g. acoustic echo cancellation. Secondly,
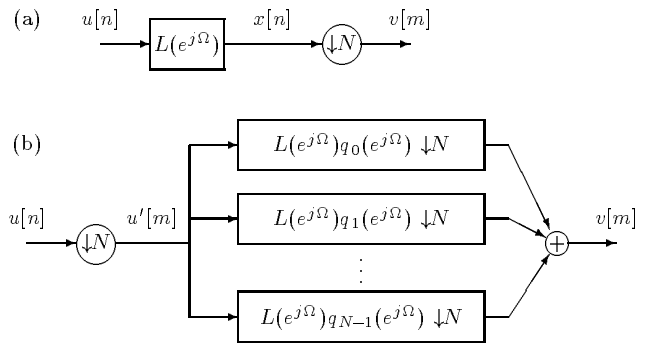

Fig. 4: The identity of the structures (a) and (b) is exploited to calculate the PSD of a decimated signal $v[m]$

for system identification applications, we state a limit for the error of the identified model.

3.1 PSD of Adapted Error Signal

Let us interpret the desired signal for the kth adaptive filter in Fig. 1 as the sum of two components,

$$d_k[m] = s_k[m] * x_k[m] + z_k[m] \quad . \qquad (3)$$

The first summand reflects the un-aliased projection of the output of the unknown system, the desired signal $d[n] = s[n] * x[n]$, into the kth subband. The second summand, $z_k[m]$, represents the aliased signal components created in the decimation stage, which can be viewed as a distortion of the LTI system and modelled as additive noise. Therefore, the Wiener solution of the kth subband filter is given by $s_k[m]$, while the unidentifiable part $z_k[m]$ defines the minimum MSE (MMSE) by [3]

$$\mathrm{MMSE} = \mathcal{E}\{z_k^2[m]\} \quad . \qquad (4)$$

To find an analytical expression for the subband MMSE, we first determine the PSD of the aliased signal parts in the subband signals, making use of two facts:

- aliasing can be conveniently pictured as a superposition of spectral intervals;

- after decimation, a previously white noise signal remains still white with identical variance.

The further proceeding is depicted in Fig. 4. Assuming the knowledge of a source model $L(e^{j\Omega})$, which is excited by a white noise signal $u[n]$, the decimation by N can be swapped with $L(e^{j\Omega})$. In each branch of Fig. 4(b) the source model is multipied with a window $q_i(e^{j\Omega})$ and then decimated by N. The windows have adjacent rectangular spectra with bandwidth $2\pi/N$ each. This decimated model is then excited by a decimated but otherwise unmodified white noise process, $u[n]$.

When we identify $v[m]$ in Fig. 4 with the desired signal $d_k[m]$, the source model for the kth subband $L_k(e^{j\Omega})$

consists of a noise shaping filter $F(e^{j\Omega})$, which represents the source model of the input signal $x[n]$ for excitation by white noise of unit variance, the unknown system $S(e^{j\Omega})$, and the analysis filter $H_k(e^{j\Omega})$,

$$L_k(e^{j\Omega}) = F(e^{j\Omega}) \cdot S(e^{j\Omega}) \cdot H_k(e^{j\Omega}) \quad . \qquad (5)$$

The PSD of $d_k[m]$ now consists of the squared sum over all N terms of the kth decimated source model in Fig. 4.

The squared sum of $N-1$ alias-only terms, defined by $N-1$ rectangular windows $q_1 \ldots q_{N-1}$ covering the stopband of the kth analysis filter $H_k(e^{j\Omega})$, finally gives the PSD of the minimum error corresponding to the MMSE,

$$S_{e_k e_k}^{\text{MMSE}}(e^{j\Omega}) = \left| \sum_{i=1}^{N-1} \sum_{n=0}^{N-1} L_k(e^{j(\Omega+2\pi n)/N}) \cdot \right.$$
$$\left. \cdot q_i(e^{j(\Omega+2\pi n)/N}) \right|^2 . \qquad (6)$$

This assumes that all un-aliased signal parts in the subband error signal $e_k[m]$ have been cancelled by the subband adaptive filter. Thus, due to the Wiener-Khintchine transform, the MMSE can be calculated as

$$\text{MMSE} = \frac{1}{2\pi} \int_0^{2\pi} S_{e_k e_k}^{\text{MMSE}}(e^{j\Omega}) d\Omega \quad . \qquad (7)$$

By inclusion of the synthesis filters $G_k(e^{j\Omega})$, it is also possible to derive the PSD of the reconstructed minimum error signal, and state the fullband MMSE analogous to (7).

Approximations. The advantage of the outlined approach is that for spectrally correlated signals, all cross-terms in the PSDs are considered. However, for weak spectral correlation, we may disregard the cross-terms between different aliased spectral intervals, and thus approximate the PSDs by swapping summations and square operations in (6). To obtain a more practical limit for the performance of SAFs, we calculate the ratio between the power levels of un-aliased and aliased subband components, creating an SNR-like measure, which we refer to as signal-to-alias ratio (SAR),

$$\text{SAR} = \frac{\int_0^{\pi/N} |P(e^{j\Omega})|^2 d\Omega}{\int_{\pi/N}^{\pi} |P(e^{j\Omega})|^2 d\Omega} \quad . \qquad (8)$$

This approximation has been based on the further assumption $F(e^{j\Omega}) = S(e^{j\Omega}) = 1$, such that (8) only depends on the magnitude response $P(e^{j\Omega})$ of the prototype filter $p[n]$. However, the SAR measure can be shown to yield valid results also for non-white input signals and unknown systems. Note that the denominator of (8) is a measure of the stopband attenuation discussed in 2.2.
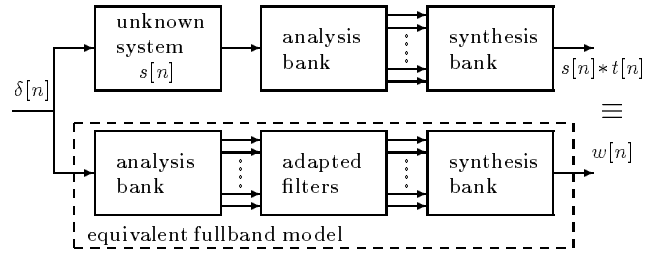

Fig. 5: Separation of system identification structure for reconstruction of equivalent fullband model.

3.2 Error of Equivalent Fullband Model

Disregarding any other limiting influences and assuming adaptation $e[n] \rightarrow 0$ in Fig. 1, an equivalent fullband model can be reconstructed from the adapted subband impulse responses $w_k[n]$ by sending an impulse through analysis bank, adapted filters and synthesis bank. A justification is demonstrated in Fig. 5 by swapping summers for the subband errors with the (linear) synthesis operation. Ideally, the fullband equivalent model $w[n]$ will match the cross-correlation function between input and desired signal, which for white noise excitation gives the unknown system $s[n]$, convolved with the distortion function $t[n]$ of the filter banks [8]. This distortion function characterizes the serial connection of the decimated filter banks in Fig. 2, $\hat{x}[n] = x[n] * t[n]$. Thus, any deviation from perfect reconstruction will result in an error in the equivalent fullband model, where the accuracy can be shown to be limited by the reconstruction error (RE),

$$\text{RE} = \|t[n] - \delta[n-L_p+1]\|_2^2 \quad . \qquad (9)$$

4 SIMULATIONS AND RESULTS

We perform adaptive system identification in a set-up as shown in Fig. 1 of a recursive system $s[n]$ with two dominant poles at $\Omega = 0.1\pi$ and 0.45π using an SAF with $K/2 = 8$ complex subbands decimated by $N = 14$. For simulation with an NLMS algorithm and strongly coloured input signal, Fig. 6 shows the PSDs of desired signal $d[n]$ and final error $e[n]$ after almost complete adaptation. In contrast, the analytically calculated PSD for the error signal at the Wiener-Hopf solution is given in Fig. 7, overlaid with the final error PSD of Fig. 6. Apart from deviations due to insufficient convergence at the band edges and residual peaks and a raised error power spectrum around the positions of the dominant poles, clearly the predicted PSD is enveloped by the simulated result, and therefore can be regarded as a lower limit of the error PSD.

Tab. 1 compares the error limits derived in Sec. 3 with simulated results for three differently designed prototypes, P_A, P_B, and P_C. The design method is a least squares minimization of stopband energy and the error in power complementarity, which can be traded off by introducing a weighting between the two measures [7].
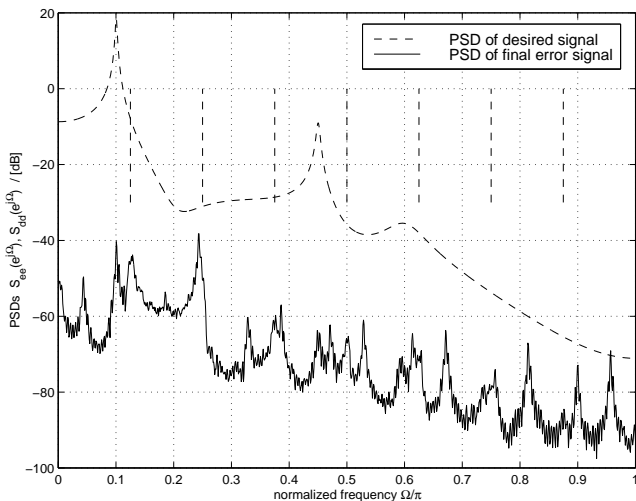
Fig. 6: PSD of desired signal and final error signal; dashed vertical lines indicate band edges.
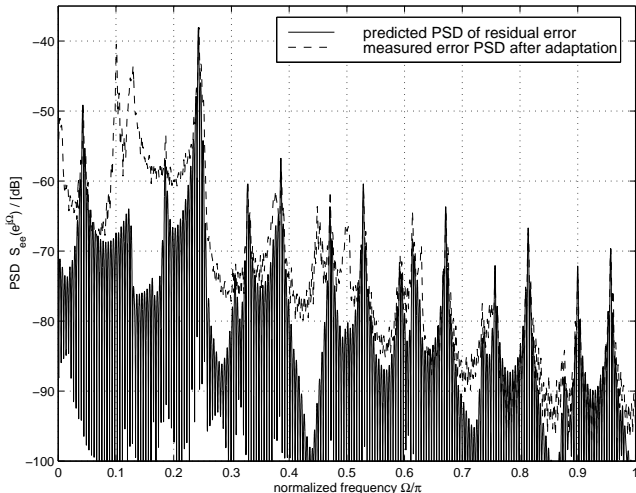

Fig. 7: PSD of final error signal and predicted PSD based on alias components in the reconstructed signal.

Tab. 1 states design results in terms of the measures RE as defined in (9) and the SAR of (8) reflecting the stopband attenuation.

For simulations, the set-up in Fig. 1 was employed to identify a delay using an RLS algorithm with white Gaussian input. The error norm of the equivalent fullband model $\|w-s\|_2^2$, where w is the reconstructed fullband model according to Sec. 3.2, is given in Tab. 1, which together with the reduction in error variance, $\sigma_{dd}^2/\sigma_{ee}^2$ fits very closely the predicted values. For the example in Fig. 6 using coloured input and a rather complex unknown system, the MSE reduction $\sigma_{dd}^2/\sigma_{ee}^2$ of 56.73dB closely agrees with an SAR value of -57.01dB for the employed prototype filter in this case.

	Analytical Prediction		Simulation Results	
	RE	SAR	$\|w-s\|_2^2$	$\sigma_{dd}^2/\sigma_{ee}^2$
P_A	-54.0821	54.9	-54.0153	54.0
P_B	-34.6191	65.2	-34.6143	66.2
P_C	-18.0016	77.8	-18.0010	78.5

Tab. 1: Predicted fullband model error and final MSE compared to simulation results (all quantities in [dB]).

5 CONCLUSIONS

We have introduced measures to predict the adaptation limits for subband adaptive filters in terms of the final MSE and the error of the identified model. In case of GDFT filter banks, they can be expressed in terms of the prototype filter, and closely agree with simulation results. For subband adaptive filter applications these measures provide convenient tools to design filter banks fulfilling pre-specified performance requirements. For applications like acoustic echo control, where the adaptation error is the most important issue, the banks can be designed to be just good (and short) enough to satisfy relaxed constraints on the model error.

6 REFERENCES

[1] R. Crochiere and L. Rabiner. *Multirate Digital Signal Processing*. Prentice Hall, 1983.

[2] A. Gilloire and M. Vetterli. "Adaptive Filtering in Subbands with Critical Sampling: Analysis, Experiments and Applications to Acoustic Echo Cancelation". *IEEE Trans. Signal Processing.*, SP-40(8):1862–1875, 1992.

[3] S. Haykin. *Adaptive Filter Theory*. Prentice Hall, 2nd ed., 1991.

[4] W. Kellermann. "Analysis and Design of Multirate Systems for Cancellation of Acoustical Echoes". *Proc. ICASSP*, 5:2570–2573, New York, 1988.

[5] D. Slock. "Fractionally-Spaced Subband and Multiresolution Adaptive Filters". *Proc. ICASSP*, 5:3693–3696, Toronto, 1991.

[6] P. Vaidyanathan. *Multirate Systems and Filter Banks*. Prentice Hall, 1993.

[7] S. Weiß, M. Harteneck, and R. Stewart. "On Implementation and Design of Filter Banks for Subband Adaptive Filter Systems". In *IEE Colloq. Digital Filters: an Enabling Technology*, London, April 1998.

[8] S. Weiß, U. Sörgel, and R. Stewart. "Computationally Efficient Adaptive System Identification in Subbands with Intersubband Tap Assignment for Undermodelled Problems". *Proc. Asilomar Conference*, 2:818–822, Monterey, CA, 1996.

[9] R. J. Wilson, P. A. Naylor, and D. Brookes. "Performance Limitations of Subband Acoustic Echo Controllers". In *Proc. IWAENC*, pp.176–179, Imperial College, London, UK, September 1997.